

Two Kuril tsunamis and analytical long wave theory

I. M. Mindlin

State Technical University of Nizhny Novgorod, Russia

E-mail address: ilia.mindlin@gmail.com

This paper addresses long waves on the water surface. It is assumed that initially the water surface has not yet been displaced from its mean level, but the velocity field has already become different from zero. This means that the motion of a body of water is triggered by a sudden change in the velocity field.

The long wave is modelled mathematically as a specific wave packet. The model is used to estimate duration of the wave origin formation, size of the origin, water elevation in the origin, energy supplied to the water by the quake, distribution of wave heights in the wave packet. Relationship between group velocity of the packet and phase velocity of the packet's wave of maximum height is revealed. These results are applied to Kuril tsunamis of November 2006 and January 2007.

Motivation of the study

Numerical study of two tsunamis triggered by the earthquakes of the 2006 and 2007 near the Kuril Islands were presented in [1]. As to comparison of the tsunamis, one can read in [1]:

1. "The dimensions of the 2007 tsunami source were smaller than those of the 2006 event, ...the 2007 tsunami had higher dominant frequency [1, p.115].
2. "The wave energy of the 2007 Kuril tsunami is reduced compared to that of 2006 Kuril tsunami" [1, p.115].
3. "at remout sites ...the ratio of 2006/2007 far-field wave heights is typically around 3:1" [1, p.115].

These three assertions, especially with the ratio 3:1, stimulate the following analytical study of gravitational water waves.

1. Problem outline.

In the present study the deep-water waves are considered which start to propagate away from an initially disturbed body of water. Then the water is acted on by no external force other than gravity. It is assumed that the free surface of the water is infinite in extent and the pressure along the surface is constant.

Referring to figure 1 and assuming that the motion is two-dimensional, in the (x, y) -plane, consider flow of an ideal heavy uniform liquid of density γ ; the x -axis is oriented upward and the y -axis in horizontal direction.

Let the curve Γ (in figure 1) be the trace of the free surface S in the (x, y) plane, $x = f < 0$, $y = 0$ be the coordinates of the pole O_1 of the polar coordinate system in the (x, y) plane, θ be the polar angle measured from the positive x -axis in the counterclockwise direction, t be the time. The external

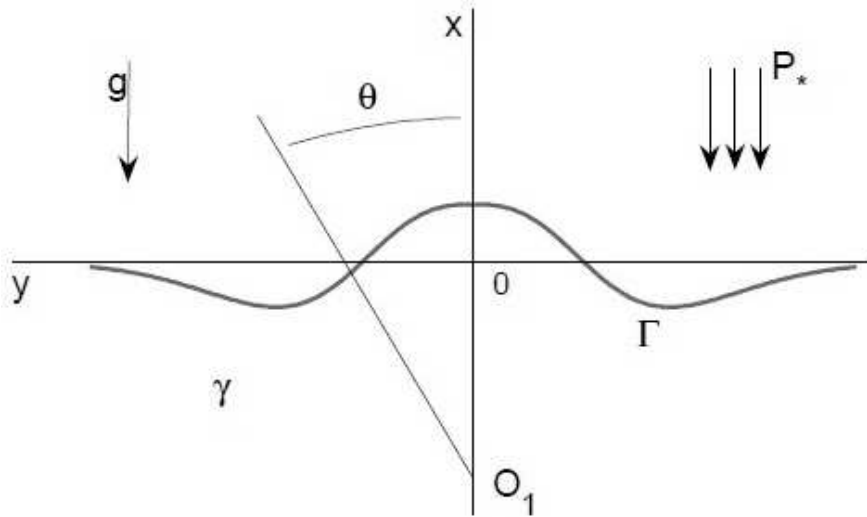


Figure 1: Coordinate systems and sketch of the free surface of a liquid.

pressure, P_* , on the free surface is constant. The liquid fills the space below the free surface. The equilibrium position of the free surface is horizontal plane $x = 0$. Assuming that the waves are generated by an initial disturbance to the water and the horizontal dimensions of the initially disturbed body of the water are much larger than the magnitude of the water surface displacement in the wave origin, equations for the water surface displacement has been obtained in parametric form [2]

$$x = cW(\theta, t), \quad y = (x - f) \tan \theta, \quad (1.1)$$

$$W = \sum_{n=1}^{+\infty} a_n T_n(\theta, \tau), \quad -\frac{\pi}{2} < \theta < \frac{\pi}{2},$$

Formulas for $T_n(\theta, \tau)$ are given in [2], the constants a_n determine initial displacement to the free surface and initial velocity field.

Formally, equations (1.1) for each specified function W describe a family of curves depending on f , t being considered as constant. The value of f determines the horizontal scale of the problem. Though the function $W(\theta, t)$ is a linear combination of the functions $T_n(\theta, \tau)$, the waves (1.1) do not obey the principle of linear superposition: the implicit form of the waves is $x = cW_0(\text{arc tangent}(y/(x - f)), t)$.

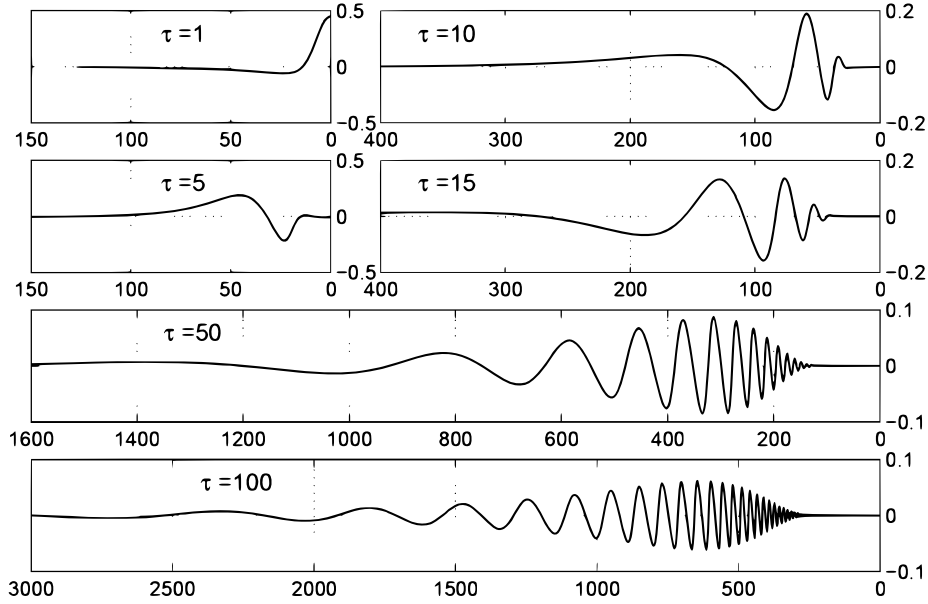


Figure 2: Profiles of the packet (2.1) at different values of τ shown in the figure near the corresponding curves, $c = 0.5$, $f = -10$.

This means that the free surface waves produced by the initial disturbance to the water is a nonlinear mixture of finite or infinite (it depends on initial conditions) set of the specific wave packets

$$x = cT_n(\theta, t), \quad y = (x - f) \tan \theta.$$

The wave packets of different numbers travel at different speed, and evolution of each packet in the mixture is not influenced by evolution of the others.

2. Theoretical model for long water waves

The surface waves are modelled by a specific wave packet

$$x = c \frac{1}{\sqrt{2|f|}} T_1(\theta, \tau), \quad y = (x - f) \tan \theta, \quad -\pi/2 < \theta < \pi/2 \quad (2.1)$$

$$T_1(\theta, \tau) = \int_0^{+\infty} x^2 e^{-x^2/2} \cos\left(\frac{1}{2}x^2 \tan \theta\right) \sin(\tau x) dx, \quad t = \tau \sqrt{2|f|}.$$

By the moment $t = 0$ the free surface has not yet been displaced from its mean level (the horizontal plane $x = 0$), but the velocity field has already become different from zero [2]:

$$T_1(\theta, 0) = 0, \quad \left. \frac{\partial T_1}{\partial \tau} \right|_{\tau=0} = 2 \cos^2 \theta \cdot \cos(2\theta)$$

Figure 2 displays profiles of the packet (2.1) at $\tau = 1, 5, 10, 15, 50, 100$.

The wave packet (2.1) travels faster than any other specific packet and with time leaves behind the other packets.

The model is adopted as a rough mathematical model for propagation of long waves through an open sea, and is not intended for detailed quantitative description of the tsunamis referred to below.

All equations are written in non-dimensional variables. Since the problem has no characteristic linear size, the dimensional unit of length, L_* , is a free parameter. But for applications in the section 6, the value of L_* , as well as the value of $|f|L_*$, will be obtained from instrumental data. The dimensional unit of time, T_* , is defined by the relation $T_*^2 g = L_*$, where g is the acceleration of free fall. The non-dimensional acceleration of free fall is equal to unity. All parameters, variables and equations are made non-dimensional by the quantities L_* , T_* , P_* and the density of water $\gamma_* = 1000 \text{ kg/m}^3$

3. Properties of the specific wave packet

Zeros of the wave packet (2.1) are defined by the equation $T_1(\theta, \tau) = 0$ and (at fixed value of τ) are situated in the numbered rays $\theta = \theta_k(\tau)$ (k is the number of a zero). Zeros $\theta_k(\tau)$ of the wave packet are independent of f .

The term 'wave' means a section of the packet which is singled out by three consecutive zeros and consists of a crest and the trough following or preceding the crest. The level difference between the crest and the trough is referred to as the wave height (or height of the wave), and the distances between two successive zeros is "half-wave-length".

At any particular moment of time, each specific wave packet contains only one wave of maximum height (WMH) on semiaxis $y > 0$ (the situation with two waves of equal maximum height can be ignored), so the zeros of WMH constitute a 'natural frame of reference' for other zeros:

Let $\theta_r(\tau)$ and $\theta_f(\tau)$ denote two of the three zeros of the WMH which correspond to minimum and maximum of the three $|\tan \theta(\tau)|$ respectively. By the zero $\theta_f(\tau)$ we define the front of WMH at the instant τ , by $\theta_r(\tau)$ the rear of the wave is determined.

Horizontal coordinate of the zero $\theta_k(\tau)$ is given by $y_k = -f \cdot \tan \theta_k(\tau)$ and the function $T_1(\theta, \tau)$ is independent of f . This leads to the following

Assertion: At any given value of τ

i) for any wave of the packet the quantity $\Delta(\tau) = h(\tau)\sqrt{2|f|}$ ($h(\tau)$ is the height of the wave) is independent of f ;

ii) the ratio of the distances $y_{k+1}(\tau) - y_k(\tau)$ and $y_k(\tau) - y_{k-1}(\tau)$ between any successive zeros of the wave packet (and, consequently, the ratio of the lengths of two successive waves) is independent of f .

Let L_* be the dimensional unit of length (in metres), then $T_* = \sqrt{L_*/g}$ is the dimensional unit of time (in seconds).

At an instant t_* the dimensional coordinate of any zero $\theta = \theta(\tau)$ is

$$y_*(t_*) = |f|L_* \cdot \tan \theta(\tau) \cdot 10^{-3} \text{ km}, \quad t_* = \tau \sqrt{2|f|} \cdot T_*/60 \text{ min},$$

and, consequently, the ratio

$$\lambda(\tau) = \frac{y_*(t_*)}{gt_*^2} = \frac{\tan \theta(\tau)}{2\tau^2} \quad (3.1)$$

depends only on τ .

When the distance is measured in kilometres and time in minutes, it is convenient to rewrite formula (3.1) as

$$\lambda_*(\tau) = \frac{y_*(t_*)}{t_*^2} \text{ km/min}^2 = 17.64 \frac{\tan \theta(\tau)}{\tau^2} \text{ km/min}^2. \quad (3.2)$$

Given a fixed value of τ , $\tan \theta(\tau)$ can be calculated from equations (2.1) of the wave packet, and corresponding value of $\lambda_*(\tau)$ can be obtained from (3.2).

Table 1 shows computed characteristics of the WMH: $\tan \theta_f$, $\lambda_*(\tau)$, and $\Delta(\tau) = H(\tau)\sqrt{2|f|}$ ($cH(\tau)$ is the maximum wave height) obtained from (2.1) and (3.2) at $c = 1$ $f = -10$).

TABLE 1. Computed characteristics of the wave of maximum height.

τ	90	100	110	120	130	140
$\tan \theta_f$	58.000	65.695	70.734	78.421	83.470	88.559
λ_*	0.1263	0.1159	0.1031	0.0960	0.0871	0.0797
$\Delta(\tau)$	0.3840	0.3661	0.3507	0.3371	0.3255	0.3152
$\lambda_* \cdot \tau$	11.368	11.589	11.343	11.528	11.326	11.158
u	0.5026	0.7695	0.5039	0.7687	0.5049	0.7606
τ	150	160	170	180	200	220
$\tan \theta_f$	96.203	101.294	108.935	116.607	126.767	142.072
λ_*	0.0754	0.0698	0.0665	0.0635	0.0559	0.0518
$\Delta(\tau)$	0.3050	0.2960	0.2884	0.2804	0.2676	0.2554
$\lambda_* \cdot \tau$	11.313	11.168	11.304	11.427	11.181	11.391
u	0.7644	0.5091	0.7641	0.7672	0.5081	0.7652
τ	240	260	280	300	310	320
$\tan \theta_f$	154.802	167.532	180.265	192.996	198.071	205.727
λ_*	0.0474	0.0437	0.0406	0.0378	0.0364	0.0354
$\Delta(\tau)$	0.2446	0.2367	0.2281	0.2204	0.2175	0.2141
$\lambda_* \cdot \tau$	11.378	11.368	11.362	11.348	11.271	11.341
u	0.6365	0.6366	0.6366	0.6365	0.5075	0.7656
τ	330	340	360	370	380	390
$\tan \theta_f$	210.802	218.458	231.189	236.267	243.920	249.002
λ_*	0.0341	0.0333	0.0315	0.0304	0.0298	0.0289
$\Delta(\tau)$	0.2108	0.2077	0.2019	0.1991	0.1965	0.1950
$\lambda_* \cdot \tau$	11.268	11.334	11.328	11.264	11.323	11.262
u	0.5075	0.7656	0.6365	0.5078	0.7653	0.5082
τ	400	410	420	440	460	470
$\tan \theta_f$	254.094	261.734	269.387	279.559	292.291	299.931
λ_*	0.0280	0.0275	0.0269	0.0255	0.0244	0.0239
$\Delta(\tau)$	0.1926	0.1902	0.1879	0.1836	0.1796	0.1776
$\lambda_* \cdot \tau$	11.205	11.261	11.314	11.208	11.209	11.257
u	0.5092	0.7640	0.7653	0.5086	0.6366	0.7640

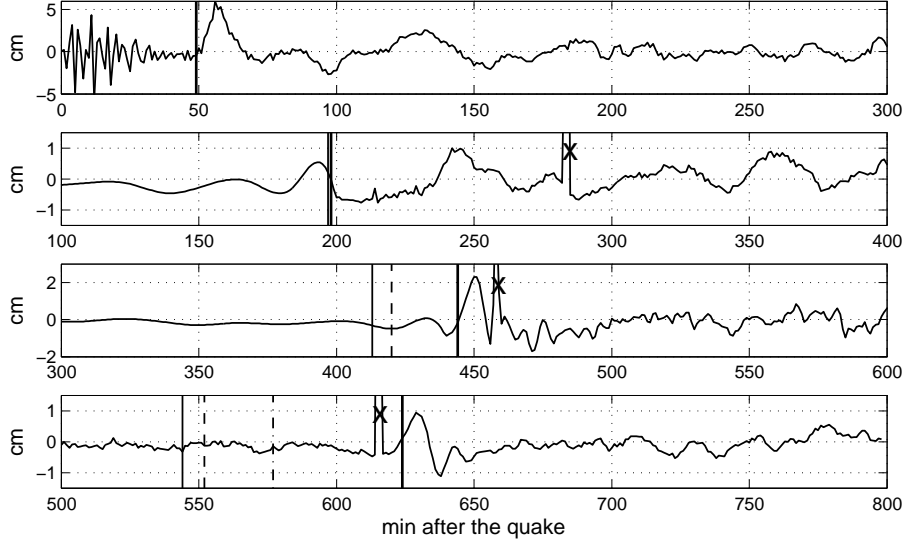


Figure 3: De-tided records of the Kuril 01/2007 tsunami at DART buoys (top to bottom) 21413, 21414, 46413, 46408, 46419.

In Table 1, values of the ratios $u = \Delta \tan \theta_f / \Delta \tau$ are given for each two neighbouring columns (for instance, for the columns $\tau = 90$ and $\tau = 100$ we find $u = (65.695 - 58.000) / (100 - 90) = 0.7695$).

During a time interval t min, the front of the WMH travels a distance $y(t)$ km at the average speed

$$V = \frac{y(t)}{t} = \lambda_*(\tau) \cdot \tau \sqrt{2|f|} \cdot \frac{T_*}{60} \text{ km/min.} \quad (3.3)$$

The value of the average speed during time interval $\Delta \tau = \tau_{n+1} - \tau_n$ equals

$$v = u \sqrt{|f| L_* g / 2} \text{ m/s,} \quad u = [\tan \theta_f(\tau_{n+1}) - \tan \theta_f(\tau_n)] / \Delta \tau, \quad (3.4)$$

where τ_n and u are given in Table 1.

The values of $\lambda_* \tau$ and u seems to suggest that the average speed of the front is nearly constant: in the interval $75 \leq \tau \leq 640$, $\lambda_* \tau$ ranges from 11.158 to 11.680.

Calculations show that the the length of the wave of maximum height equals to

$$l = L_* |f| (\tan \theta_f - \tan \theta_r) \approx 5 L_* |f| \quad \text{for } 30 < \tau < 640. \quad (3.5)$$

4. Gauge records and data extracted from the records

Data of 2006 Kuril and 2007 Kuril tsunamis generated by the earthquakes of the 15 November 2006 and the 13 January 2007, respectively, are used to test the theory.

The data is obtained from tsunami records at DART buoys (DART - Deep-ocean Assessment and Reporting of Tsunami) deployed in the Pacific Ocean at a depth of 5000 metres. Waves arriving at a deep-ocean buoy is a mixture of tidal, seismic, and gravity waves which come from the tsunami origin itself. Records of the buoys and their locations can be found on the USA National Data Buoy Center public website (<http://www.ndbc.noaa.gov/dart.shtml>).

Figure 3 shows the Kuril 01/2007 tsunami records de-tided using low-pass Butterworth filter with 150 min cut-off.

Data extracted from the records at the DARTs are summarized in Tables 2 - 3, where the travel time of the MHW, t_* min, the maximum wave-height, H_* cm, and the distance between the gauge sensors and the centre (epicentre of the earthquake) of the wave origin, y_* km, are shown for each of the DARTs.

TABLE 2. The 2007 Kuril tsunami: WMH as recorded at the DART buoys.

	buoy	DART	t_* min.	H_* cm	y_* km	y_*/t_*^2
Data 1.	1	21413	120	4.0	1762	0.122361
	2	21414	120	5.7	1804	0.125278
	3	46413	154	5.7	2253	0.094999
	4	46408	200	4.5	2660	0.066500
	5	46419	438	1.6	5470	0.028513

TABLE 3. The 2006 Kuril tsunami: WMH as recorded at the DART buoys.

	buoy	DART	t_* min.	H_* cm	y_* km	y_*/t_*^2
Data 2.	1	46413	155	8.5	2331	0.097024
	2	46408	238	7.5	2735	0.048284
	3	46402	270	10.0	3127	0.042894
	4	46403	365	7.5	3581	0.026879

5. Theoretical characteristics of the WMH

The Table 1 shows that $\tan \theta_f$ and λ_* are monotone functions of τ , so for given value of λ_* the values of τ and $\tan \theta_f$ can be calculated using equations (2.1) or estimated using Table 1.

For each DART location, setting $\lambda_* = y_*/t_*^2$ (see Tables 2 - 3) and using Table 1, we obtain the results, shown in Tables 4 - 5. Values of τ , $\tan \theta_f(\tau)$, $\Delta(\tau)$ in the first line of Table 4 are obtained with the use of $\lambda_* = 0.122361$ (in the first line of Table 2) and Table 1 as follows. We see from Table 1 that $0, 1159 < \lambda_* = 0, 122361 < 0, 1263$, $90 < \tau < 100$, $58.000 < \tan \theta_f(\tau) < 65.695$, $0, 3661 < \Delta(\tau) < 0.3840$.

Linear interpolation gives $\tau = 93.787$, $\tan \theta_f(\tau) = 60.914$, $\Delta(\tau) = 0, 374984$. The rest lines in Table 4 are obtained in the same way.

Table 4. For Data 1: theoretical characteristics of the WMH at locations of DART buoys.

buoy	λ_*	τ	$\tan \theta_f(\tau)$	Δ
1	0.122361	93.787	60.914	0.374984
2	0.125278	90.983	58.756	0.378995
3	0.094999	121.125	78.987	0.335795
4	0.066500	170.000	108.935	0.288400
5	0.028513	394.300	251.192	0.193968

Table 5 is similar to Table 4 and obtained in similar way.

Table 5. For Data 2: theoretical characteristics of the WMH at locations of the DART buoys.

buoy	λ_*	τ	$\tan \theta_f(\tau)$	Δ
1	0.097024	118.558	78.411	0.339047
2	0.048284	235.888	154.791	0.246741
3	0.042894	265.038	180.234	0.234534
4	0.026879	420.300	279.545	0.187836

6. Estimators for the wave model parameters

For the front of the wave of maximum height (as for any zero) the following formulas hold

$$y_*(t_*) = -f \tan \theta_f(\tau) \cdot L_* > 0, \quad t_* = \tau \sqrt{2|f|L_*/g}.$$

If at each locality i data for the waves (2.1) were obtained from the records exactly, the functions

$$S(a) = \sum_i (y_{*i}(t_{*i}) - a \cdot \tan \theta_{1i}(\tau_i))^2 \quad \text{and} \quad F(a) = \sum_i \left(60t_{*i} - \tau_i \sqrt{\frac{2a}{g}} \right)^2$$

would be equal to zero at $a = |f_*|$, where $|f_*| = |f|L_*$.

But using equations (2.1) and values of y_{*i} , t_{*i} , H_{*i} (obtained with errors) we estimate the value of a by minimizing $S(a)$ or $F(a)$.

Minimum value of $S(a)$ occurs at

$$a = |f_{*1}| = \frac{\sum_i y_{*i} \tan \theta_{1i}}{\sum_i \tan^2 \theta_{1i}} \text{ km}, \quad (6.1)$$

while minimum value of $F(a)$ is reached at

$$a = |f_{*2}| = \left(\frac{\sum_i t_{*i} \tau_i}{\sum_i \tau_i^2} \cdot 60 \right)^2 \text{ 4.9 m.} \quad (6.2)$$

In the Table 1, the quantity $\Delta(\tau) = H(\tau) \sqrt{2|f|}$ is independent of f ($cH(\tau)$ is the height of the WMH). If the data in Tables 2 - 4 were measured exactly at each locality i , the function

$$R(s) = \sum_i (c\Delta(\tau_i) \frac{1}{\sqrt{2|f|}} L_* - H_{*i})^2 = \sum_i (\Delta(\tau_i)s - H_{*i})^2, \quad s = \frac{c}{\sqrt{2a}} L_*^{3/2}$$

would be equal to zero at true value of s .

At actual values of H_{*i} the value of s is estimated by minimizing $R(s)$, which leads to the estimator

$$c^2 L_*^3 = 2a\eta^2, \quad \eta = \frac{B}{A}, \quad A = \sum_i \Delta^2(\tau_i), \quad B = \sum_i \Delta_i H_{*i}, \quad (6.3)$$

where η is independent of c and f , a is estimated by (6.1) or (6.2).

For Data 1, Tables 2 and 4, estimators (6.1), (6.2), and (6.3) give

$$a_1 = 23.413 \text{ km}, \quad a_2 = 23140 \text{ m}, \quad \eta = 13.8 \text{ cm}.$$

Tables 3 and 5 (for Data 2) lead to the values

$$a_1 = 15.424 \text{ km}, \quad a_2 = 15785 \text{ m}, \quad \eta = 54.8 \text{ cm}.$$

7. Estimation of the wave origin parameters

7.1. Dimensions of the wave origin

Here, the water surface above the disturbed body of water is referred to as the wave origin.

By model (2.1), at the moment $t = 0$ the free surface has not yet been displaced from its mean level (the horizontal plane $x = 0$), but the velocity field has already become different from zero.

Calculations show that during some time interval, say $0 \leq \tau \leq \tau_1$, a water hill in the form of a rounded solitary elevation symmetric with respect to the vertical x -axis is appearing on the water surface (Fig. 2). For the model (2.1), the height of the hill increases and reaches the maximum at $\tau = \tau_1 = 0.872$. On the interval $0 \leq \tau \leq \tau_1$ there is only one zero $\theta(\tau)$ in the water surface (at $y > 0$), and the zero is almost immovable. Only at $\tau > \tau_1$ the heap of water begins to spread out and to turn into a wave group, which runs away from the wave origin. The time interval $0 \leq \tau \leq \tau_1$ is referred to as the interval of formation of the wave origin.

The quantity $a = |f|L_*$ is the characteristic horizontal scale of the wave origin, so we determine the effective length, l_{ef} , of the origin by $l_{ef} = ka$. The body of water in the region $|y| < l_{ef}$ may be referred to as effective wave origin.

The value of k may be assigned to meet different conditions; for instance, at $t = 0$ the energy of the water outside the effective origin does not exceed 5% of the total wave energy or the magnitude of the sea surface displacement at the margin of the effective wave origin does not exceed a given value.

It is found from (2.1), that the maximum free surface displacement on the boundary of the wave originating area is given by

$$W_b = \frac{1}{\sqrt{2|f|}} T_1(\theta_b, \tau_1), \quad \tau_1 = 0.842.$$

The quantity $-h_b = \sqrt{2|f|} W_b$ is independent of f . The values of the quantity corresponding to different values of $k = \tan \theta_b$ are shown in Table 6.

Table 6. Values of $-h_b$ corresponding to some values of k .

k	3.0	3.5	4.0	4.5	5.0	5.5	6.0
$-h_b$	0.1137	0.0953	0.0795	0.0666	0.0563	0.0480	0.0413
k	6.5	7.0	8.0	9.0	10.0	11.0	12.0
$-h_b$	0.0358	0.0314	0.0245	0.0197	0.0161	0.0134	0.0113

For the model (2.1), $W_b < 0$ at $k > 1.3$ (Fig. 2).

7.2. Water elevation in the wave origin.

Calculations show that $\max \Delta(\tau) = \Delta(0.842) = 1.036$ (the maximum is reached at $\theta = 0$). This means that the maximum of the water elevation, h , in the wave origin is given as

$$h = 1,036cL_* \frac{1}{\sqrt{2|f|}} = 1.036\eta \text{ cm.} \quad (7.1)$$

where η is given by (6.3).

Formulas (6.3) and (7.1) lead to the following estimates:

$$\eta_1 = 13.8 \text{ cm, } h_1 = 14.3 \text{ cm; } \eta_2 = 54.8 \text{ cm, } h_2 = 56.7 \text{ cm,} \quad (7.2)$$

where the subscripts 1 and 2 correspond to the Data 1 (the 2007 Kuril tsunami) and Data 2 (the 2006 Kuril tsunami) respectively.

The ratio $\Delta_b/1.036$ is the ratio of water surface displacement on the boundary of the wave origin to the maximum water displacement in the wave origin.

7.3. Duration of wave origin formation.

Duration t of the wave origin formation is estimated by ($g = 9.8 \text{ m/s}^2$, a is measured in metres)

$$t = 0,842\sqrt{2a/g},$$

which gives $t = 58 \text{ s}$ for Data 1, and $t = 47 \text{ s}$ for Data 2.

7.4. Estimation of the waves energy

It is supposed above, initially still water is set in motion at $t = 0$ by an impulsive force. Kinetic energy supplied to the water by the force can be estimated by integral (involving velocity potential and its normal derivative) evaluated over the sea surface [3]

The energy supplied to the vertical layer of the water between two parallel planes at the distance $a = |f|L_*$ apart is given by

$$E = \frac{1}{8}\pi|f|c^2 \cdot \gamma g L_*^4 \text{ J} = \frac{1}{4}\pi\gamma g a^2 \eta^2 \text{ J.} \quad (7.3)$$

With the values of a and η obtained in sections 5 and 7.2, we find the energy estimates as

$$E_1 = 5.03 \cdot 10^{10} \text{ J, } E_2 = 1.87 \cdot 10^{11} \text{ J, } E_2 = 3.72E_1 \quad (7.4)$$

The subscripts 1 and 2 correspond to the Data 1 and Data 2 respectively.

Estimates (7.4) are in line with the second quotation from [1] given above.

8. Theoretical estimation of waves parameters

8.1. Estimation of the WMH length

By (3.5) the WMH have the lengths $l \approx 5a$

$$l_1 \approx 117 \text{ km}, \quad l_2 \approx 76 \text{ km}$$

obtained from Data 1 and 2 respectively.

The smaller value of a , the smaller effective size $l_{ef} = ka$ of the wave origin and wave length, the higher dominant frequency of the WMH.

These results are in line with the first quotation from [1] given above.

8.2. Speed of the wave of maximum height.

For the 2007 Kuril tsunami, using data of Table 2, we find that actual values of average speed of the front of WMH (during time interval $0 - t_*$) arrived at the buoys locations are

$$V_{*1} = \frac{1762 \cdot 60}{120} = 881 \text{ km/h}, \quad V_{*2} = 902 \text{ km/h},$$

$$V_{*3} = 878 \text{ km/h}, \quad V_{*4} = 798 \text{ km/h}, \quad V_{*5} = 749 \text{ km/h}$$

with arithmetic mean 838 km/h.

We introduce the notation $a(\text{m}) = 20$ which means that the number 20 is nondimensionl while a is measured in metres: $a = 20 \text{ m}$.

The travel time t_* is estimated as

$$t_* = \frac{\tau}{60} \cdot \sqrt{\frac{2a(\text{m})}{9.8}} \text{ min.} \quad (8.1)$$

By (3.2) and (8.1) the group velocity of the packet (2.1) is

$$V \text{ km/min} = \frac{y_*}{t_*} = \lambda_* t_* = \lambda_* \tau \text{ km/min}^2 \cdot \frac{1}{60} \sqrt{\frac{2a(\text{m})}{9.8}} \text{ min.}$$

Substituting $a = l/5l$ $\lambda_* \tau \approx 11.3$ (from Table 1) we obtain the relation between the group velocity and the length of the wave of maximum height as

$$V_* \approx 11.3 \frac{1}{\sqrt{4.9 \cdot 3.6 \cdot 5}} \sqrt{l(\text{km})} \text{ km/min}$$

or

$$V_* = 1.22 \sqrt{l(\text{km})} \text{ km/min.} \quad (8.2)$$

At $l = 117$ km formula (8.2) gives $V_* = 13.20$ km/min = 792 km/h.

Instantaneous speed of the wave of maximum height is estimated as

$$v_* = uT_* = u\sqrt{2ag} = u\sqrt{17.6a(\text{m})} \text{ m/s.}$$

where a is measured in metres, $g = 9.8$ m/s².

When a is measured in kilometres and time in minutes we get

$$v_* = uT_* = u\sqrt{17.6 \cdot 3.6} \sqrt{a(\text{km})} \text{ km/min.}$$

Substituting $a = l/5$ and taking $u = (0.50 + 0.76)/2$ (from Table 1) we obtain

$$v_* = 2.24 \sqrt{l(\text{km})} \text{ km/min.} \quad (8.3)$$

The ratio of the wave group speed to the instantaneous speed of the wave of maximum height is

$$\frac{V_*}{v_*} = \frac{1.22}{2.24} = 0.54$$

at any length of WMH.

Phase velocity c of harmonic waves on deep water and their wave length are related as

$$c = \sqrt{\frac{gl}{2\pi}} \text{ m/s} = \sqrt{\frac{9.8 \cdot 3.6}{2\pi}} \sqrt{l(\text{km})} \text{ (km/min)} = 2.37 \sqrt{l(\text{km})} \text{ (km/min).}$$

The wave group speed of packet (2.1) is a half of the phase velocity of harmonic wave when the packet's wave of maximum height and the harmonic wave have equal lengths: $\frac{V}{c} = \frac{1.17}{2.37} = 0.493$.

In passing. By the linear theory, speed c of harmonic waves, their wavelength l , and d , the uniform depth of the water, are related as follows

$$c^2 = \frac{gl}{2\pi} \tanh \frac{2\pi d}{l}.$$

For Data 1 the length of the wave of maximum height is 117 km, its speed $V = 792$ km/h = 220 m/s.

At these values we get

$$\tanh \frac{2\pi d}{l} = 0,259, \quad \frac{2\pi d}{l} = 0,27, \quad d = 5030 \text{ m,}$$

which is in line with the depth of the Pacific ocean.

8.3. Distribution of the wave heights in the packet (2.1)

The height of the wave of number k in the packet (2.1) is estimated as

$$H^* = |x_{max} - x_{min}| = c \frac{\Delta_k \cdot L_*}{\sqrt{2|f|}} = c\Delta_k \sqrt{\frac{L_*^3}{2|f_*|}} = \Delta_k(\tau)\eta. \quad (8.4)$$

For the wave of MH the value of $\Delta_k(\tau) = \Delta(\tau)$ is shown in Table 1.

With time in the packet a central part is developing which contains waves of nearly equal heights. One can see the central part in the interval $250 < y < 400$ at $\tau = 50$ and in the interval $500 < y < 700$ at $\tau = 100$ (fig. 2). With time the length of the central part increases. In the central part $\Delta_k(\tau) \approx \Delta(\tau)$ shown in Table 1.

It was found above from data 1 that $\eta_1 = 13.8$ cm and $\eta_2 = 54.8$ cm from data 2. By (8.4) the maximum wave heights are estimated as $H_1^* = 13.8\Delta(\tau)$ cm for data of 2007 and $H_2^* = 54.8\Delta(\tau)$ cm for data of 2006. The ratio of the maximum wave heights $H_2^*/H_1^* = 3.96$, so the ratio of wave heights in the central parts of the tsunami waves approximately equals 3.96.

The ratio is equal 3.96, if the wave heights are taken at the same value of τ . Under this condition, from (8.1) and (3.1) we get

$$\frac{t_{*2}}{t_{*1}} = \sqrt{\frac{a_2}{a_1}} = \sqrt{\frac{y_{*2}}{y_{*1}}}. \quad (8.5)$$

where the subscripts 1 and 2 correspond to Data 1 (the 2007 Kuril tsunami) and Data 2 (the 2006 Kuril tsunami) respectively.

It follows from (3.5) and (8.5) that

$$\frac{y_*}{a} = \frac{5y_*}{l},$$

$$\frac{y_{*2}}{l_2} = \frac{y_{*1}}{l_1} = n, \quad \frac{t_{*2}}{t_{*1}} = \sqrt{\frac{a_2}{a_1}}. \quad (8.6)$$

When the conditions (8.6) are satisfied approximately the ratio of the maximum wave heights $\frac{H_2^*}{H_1^*}$ of the Kuril tsunamis may be greater or less than 3.96.

It seems in [1] the calculations were performed at proper values of time and at proper numbers of waves (of crests).

This result agrees with the third quotation from [1].

9. Theoretical forecast for the waves recorded.

In Table 2 the darts are arranged from top to bottom according to their arrival time.

Consider the situation when the first two lines in Table 2 are known, but the records of the next three buoys are not obtained yet.

Bellow, starting from the first two lines of Table 2, a line of forecasts of the WMH arrival time and amplitude at the next three buoys is produced corresponding to the timeline of the DART records.

For each of the next three buoys $\tan \theta_f = y_*/a$ is calculated, which is then used to locate the values of τ and Δ between two appropriate consecutive values from Table 1.

Then, for each buoy, the travel time of the WMH and its height at the locations of the buoys are estimated by (8.1) and (8.4)

9.1. The forecast based on Data 1

The forecast based on two DART records.

The first two lines of Table 2, the first two lines of Table 4, and formulas (6.1) and (6.3) give

$$a = |f_{*1}| = 29.783 \text{ km}, \quad A = 0,28425, \quad B = 3,066208 \text{ cm} \quad \eta = 12.877 \text{ cm}$$

For the buoy 3 we obtain

$$\tan \theta_f = \frac{y_*}{a} = \frac{2253}{29.783} = 75.648.$$

From Table 1 we see that $70.734 < 75.648 < 76.421$. This gives intervals for τ and Δ :

$$110 < \tau < 120, \quad 0.3371 < \Delta < 0.3607$$

Linear interpolation gives the estimates $\tau = 116,3921$, $\Delta = 0,342007$.

The travel time of the WMH and its height at the location of the buoy 3 are estimated by (8.1) and (8.2) (a is taken in metres) as

$$t^* = 151 \text{ min}, \quad H^* = 4.4 \text{ cm}$$

For buos 4 and 5 we get

$$\tan \theta_f = \frac{y_*}{a} = \frac{2660}{29.783} = 89.313, \quad \tan \theta_f = \frac{y_*}{a} = \frac{5470}{29.783} = 183.663$$

The forecast for the buoys 4 and 5 is obtain on the same lines as for buoy 3.

Table 7. For Data 1: the forecast based on two DART records.

Buoy	$\tan \theta_f$	τ	Δ	t^* min	H^* cm
3	75.785	116.570	0.341764	151	4.4
4	89.313	140.987	0.314194	183	3.4
5	183.663	285.338	0.223815	370	2.9

The forecast based on three DART records. The following forecast is based on the measurements on DART buoys 21413, 21414, and 46413.

The first three lines of Table 2, the first three lines of Table 4, and formulas (6.1) and (6.3) give

$$a = |f_{*1}| = 29.197 \text{ km}, \quad \eta = 14.04 \text{ cm}.$$

Table 8. For Data 1: the forecast based on three DART records.

Buoy	$\tan \theta_f$	τ	Δ	t^* min	H^* cm
4	91.116	143.305	0,311829	184	4.4
5	183.305	291.131	0.223815	374	3.1

The forecast based on four DART records. The following forecast is based on the measurements on DART buoys 21413, 21414, 46413, and 46408.

The first four lines of Table 2, the first four lines of Table 4, and formulas (6.1) and (6.3) give

$$a = |f_{*1}| = 26,952 \text{ km}, \quad \eta = 10.926 \text{ cm}.$$

Table 9. For Data 1: the forecast based on four DART records.

Buoy	$\tan\theta_f$	τ	Δ	t^* min	H^* cm
5	202.949	316.371	0,215841	390	2.1

For Data 1, the results are summarized in Tables 10 where for each of the mentioned DART buoy's locations the forecast of travel time t_k^* (in minutes) of the wave of maximum height and its height H_k^* (in centimetres) are shown; the subscript k shows that the forecast is based on measurements obtained from k buoys.

The actual travel time t_* and height H_* are repeated from Table 1.

Table 10. For Data 1: the forecasts based on the model (2.1).

Buoy	t_2^*	t_3^*	t_4^*	t_*	H_2^*	H_3^*	H_4^*	H_*
3	151	-	-	154	4.4	-	-	5.7
4	183	184	-	200	3.4	4.4	-	4,5
5	343	374	390	438	2.9	3.1	2.4	1,6

In figure 3 vertical lines mark the arrival of the front of the WMH (thick solid line), its estimate with the first and second buoy records for the next three buoys (thin solid), its estimate with the first three buoy records for the next two buoys (dashed), its estimate with the four buoys for the last one (dashdot). Cross marks a trigger pulse (signals send by an operator).

9.2. The forecast based on Data 2

The Data 2 obtained from the records are shown in Table 4. The results of forecasting are presented in Table 11.

Table 11. For Data 2: the forecasts based on the model (2.1).

Buoy	t_1^*	t_2^*	t_3^*	t_*	H_1^*	H_2^*	H_3^*	H_*
2	187	-	-	238	7.8	-	-	7.5
3	214	257	-	270	7.3	6.6	-	10.0
4	243	295	307	365	6.9	6.2	6.8	7.5

Discussion

1. When the above estimates for a hypothetical tsunami are applied to actual tsunamis one should keep in mind that the estimates may be reliable only for far-field sites since the DARTs are situated at long distances from the tsunami source.

2. Figures (7.4) underestimate the actual energy of the Kuril tsunamis as the energy flux depends on azimuthal direction.

Modelled energy fluxes for the Kuril tsunamis were directed southeastward from the source areas, in the direction of the Havaian Islands and Peru-Chile [1]. while all DARTs named in the Tables 2 and 3 are situated in the direction of Alaska.

Also underestimation of water elevation in the wave origin has resulted from the discrepancy between the directions.

3. The figures (7.4) may be interpreted as estimates of the wave energy radiated in a sector containing the DARTs. That is why our present results shows good agreement with those obtained in [1] and the predicted arrival times and predicted wave heights are comparable with that obtained from the records.

4. It is unusual that long waves may be considered in the water of infinite depth. But the answer to a problem depends on its formulation.

The problem on gravitational wave on infinite water surface must involve conditions at infinity along the surface. In the linear theory of water waves (no matter the water depth is finite or infinite) speed of the waves along the water surface should be bounded by a constant. This condition leads to solution in the form of sinusoidal waves. Sinusoidal waves require the energy supplied to the water by a source of disturbances to be infinite.

In the theory of specific wave packets the energy supplied to the water is finite at any moment of time. Consequently, periodic waves on the free surface infinite in extent (including sinusoidal and progressive Stokes waves) are 'prohibited' by this condition.

The energy supplied to the water by a quake is finite. This may explain the fact that the speed of tsunami in an open sea and group speed of the packet (2.1) are almost the same.

REFERENCES

1. A.B.Rabinovich, L.I.Lobcovsky at all, Near source observation and modelling of the Kuril Iseland tsunamis of 17 november 2006 and 13 January 2007. Adv.Geosci, 4,105-116, 2008/ www.adv-geosci.net/14/105/2008.
2. Mindlin, I.M., Deep-water gravity waves: nonlinear theory of wave groups. arXiv:1406.1681v1 [physics.ao-ph], 30 p, (6 Jun 2014)
3. Miln-Thomson, L.M., Theoretical Hydrodynamics, Macmillan and Co. LTD, London, 1960.